Theoretical Study of the Substrate Mechanism of Ribonucleotide Reductase

Per E. M. Siegbahn

Contribution from the Department of Physics, Stockholm University, Box 6730, S-113 85 Stockholm, Sweden

Received October 16, 1997. Revised Manuscript Received May 18, 1998

Abstract: The substrate mechanism of ribonucleotide reductase (RNR) is studied using a hybrid DFT method (B3LYP) with large basis sets. With models for the calculations based on recently determined X-ray structures, different mechanisms of the steps leading from a ribonucleotide to a deoxyribonucleotide are investigated. It is suggested that the transformation occurs in six steps. The role of the amino acid residues present at the active site are studied in detail. Three cysteine residues are known to be necessary for the formation of a deoxyribonucleotide, but very recently a glutamic acid residue has also been shown to be essential. The calculations indicate that this glutamic acid residue, Glu441, is important both in steps 2 and 4. In the suggested step 2, Glu441 transfers a hydrogen from the C3′-OH group to the C2′-OH group, and in step 4 it is proposed to participate in a cyclic transition state bridging the carbon and oxygen atoms of a keto group at C3′. In both these steps an asparagine, Asn437, also plays an important role in reducing the barrier heights for the reactions. The rate-limiting step of the substrate reactions is suggested to be step 4, where a cysteine residue attacks the C3′ center of the ribose ring. The disulfide bond is proposed to be formed in step 5. Dielectric effects from the surrounding protein are very small and of almost no importance in this process.

I. Introduction

DNA differs chemically from RNA in two major respects. First, its nucleotides contain 2′-deoxyribose residues rather than ribose residues. Second, DNA contains the base thymine, whereas RNA contains uracil. The present study concerns the mechanism for the first of these reactions, shown in Scheme 1. The enzymes that catalyze the set of reactions required for the transformation are named ribonucleotide reductases (RNR). Three classes of RNR have been characterized. The present study concerns the class I enzymes for which a tyrosyl radical is produced by an oxo-bridged binuclear iron complex. The *Escherichia coli* RNR has been shown to be an $\alpha_2\beta_2$ tetramer that can dissociate into two catalytically inactive homodimers, R1 and R2.[1] The formation of the tyrosyl radical by the iron center occurs in R2 while the substrate reactions occur in R1. The X-ray structures of both R1 and R2 have been determined, the one of R2 by Nordlund, Sjöberg, and Eklund[2] and the one of R1 by Uhlin and Eklund.[3] Very recently, the structure of R1 including a substrate was also determined, by Eriksson et al.[4] These structures indicate that the distance between the active site in R1 and the tyrosyl radical, Tyr122, in R2 is as large as 30−40 Å and that a chain of conserved hydrogen bonded residues connects these sites.[3,5]

The mechanism by which the iron dimer center produces the tyrosyl radical and the chemical mode of the subsequent communication between the radical site in R2 and the substrate site in R1 are subjects of intense present research,[5,6] but these points will not be discussed further here. Instead, the present study starts at the point where the Cys439 radical at the substrate site is formed.

Scheme 1

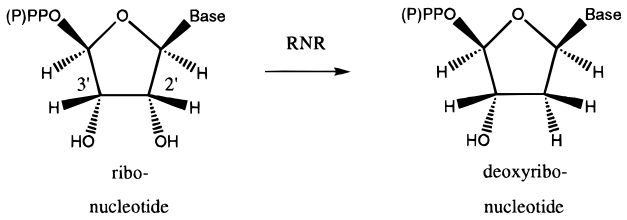

The region around the substrate is shown in Figure 1, which is taken from the X-ray structure.[3] The more recent X-ray structure with a bound substrate[4] indicates that the ribonucleotide is bound by hydrogen bonds to its hydroxyl oxygen atoms. These hydrogen bonds are formed to Glu441 at the C3′-oxygen and to a combination of Glu441 and Asn437 at the C2′-oxygen. Three cysteines in this region are furthermore critical for the substrate reactions. Cys439 is connected by a 30-Å-long hydrogen-bonded chain to Tyr122, as already mentioned. Two other cysteines, Cys225 and Cys462, form a disulfide bond during the substrate reactions and are therefore also essential.

On the basis of isotopic labeling and kinetic, spectroscopic, and site-directed mutagenesis experiments, a reaction mechanism has been suggested by Stubbe et al.[7,8] consisting of the steps shown in Scheme 2. In this scheme, S_A stands for Cys439, S_B for Cys225 and S_C for Cys462. In the first step a hydrogen

(1) Reichard, P. *Science* **1993**, *260*, 1773−1777.
(2) Nordlund, P.; Sjöberg, B.-M.; Eklund, H. *Nature* **1990**, *345*, 593−598.
(3) Uhlin, U.; Eklund, H. *Nature* **1994**, *370*, 533−539.
(4) Eriksson, M.; Uhlin, U.; Ramaswamy, S.; Ekberg, M.; Regnström, K.; Sjöberg, B.-M.; Eklund, H. *Structure* **1997**, *5*, 1077−1092.
(5) Sjöberg, B. M. *Structure* **1994**, *2*, 793−796. Sjöberg, B.-M. *Struct. Bond.* **1997**, *88*, 139−173.
(6) Gräslund, A.; Sahlin M. *Annu. Rev. Biophys. Biomol. Struct.* **1996**, *25*, 259−286.
(7) Stubbe, J. *Biol. Chem.* **1990**, *265*, 5330.
(8) Mao, S. S.; Holler, T. P.; Yu, G. X.; Bollinger, J. M.; Booker, S.; Johnston, M. I.; Stubbe, J. *Biochemistry* **1992**, *31*, 9733−9743.

S0002-7863(97)03606-8 CCC: $15.00
Published on Web 08/07/1998

Scheme 2

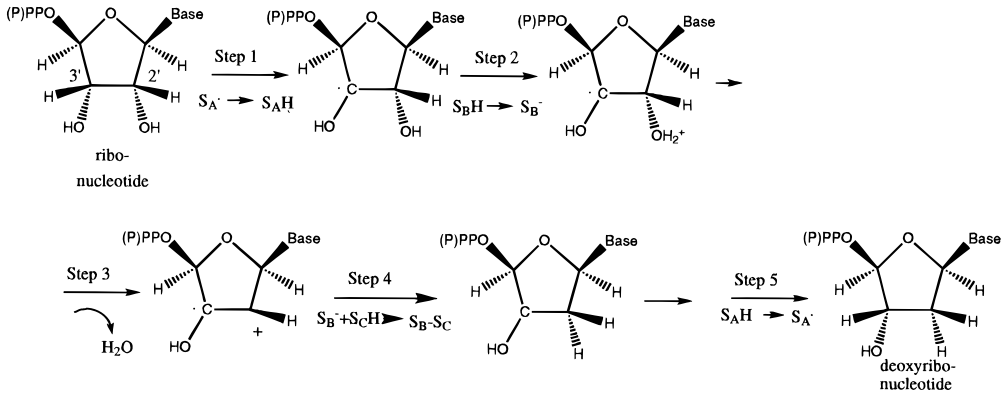

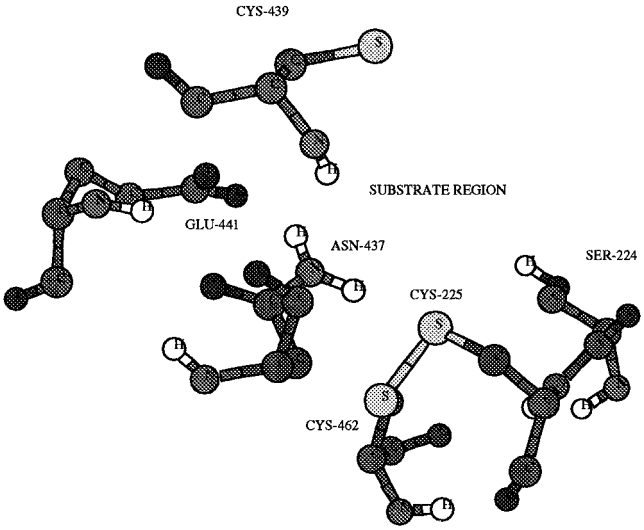

Figure 1. X-ray structure of the substrate region of the R1 subunit of *E. coli* RNR

atom from C3′ of the ribonucleotide substrate is abstracted by the Cys439 radical mentioned above. In the second step, a proton is abstracted by the C2′-hydroxyl of the substrate from a cysteine, plausibly from Cys225, leaving the substrate as a protonated radical species and the cysteine as an anion. In the third step, a water molecule leaves the substrate. In the later, slightly modified mechanism,[8] an initial carboxylate anion simultaneously abstracts a proton from the C3′-hydroxyl group, leading to a neutral substrate radical at the end of step 3. In the fourth step, a hydrogen atom is abstracted by C2′ of the substrate from a cysteine. An electron is also transferred to the substrate from the cysteines, while a disulfide bridge is simultaneously formed between Cys225 and Cys462. In the modified scheme an electron is transferred to the carboxylate group simultaneously with a proton transfer from the carboxylate to the C3′-oxygen of the keto group. This leaves the substrate as a C3′-radical, which in the fifth step can reabstract a hydrogen atom from Cys439 to complete the cycle and the formation of the deoxyribonucleotide product. Many of these steps are chemically quite complicated, in particular the ones where water and the disulfide bridge are formed, and it is clear that some of these suggestions must be regarded as tentative. The present theoretical study uses the suggested mechanism in Scheme 2 as a starting point to test different possibilities. The model is then extended on the basis of the X-ray structures of R1 and finally a new mechanism is suggested. The new mechanism has many similarities, but also a number of significant differences from the suggested mechanism in Scheme 2.

Two recent studies related to the mechanism of the substrate reaction of RNR will also be mentioned. The first of these is an experimental model study by Lenz and Giese,[9] where a C3′-radical is generated by photolysis. It was shown that starting with this radical, elimination of the C2′-OH group readily takes place under general base catalysis, providing support for the first two steps of the mechanism in Scheme 2. In the second recent study mentioned here, by Persson et al.[10] the Glu441 residue was replaced by other residues via site-directed mutagenesis. It was shown that the carboxylate side chain in Glu441 is essential for keeping turnover activity. The only mutation which still showed activity was one where the glutamate was replaced by an aspartate. When Glu441 was replaced by a glutamine only half a turnover occurs. Two transient consecutive radicals were observed, one of which tentatively assigned as the C3′-radical shown in Scheme 2. Further references relevant to the present study, can be found in recent reviews.[5,6]

The method used in the present study is the same as has been used in other recent studies of biochemical reactions.[11] This method, termed B3LYP, is a DFT (density functional theory) method based on hybrid functionals containing both gradient corrections and Hartree−Fock exchange.[12] Three parameters are included fitted to experiments. Benchmark tests show that this method is almost as accurate as the most accurate ab initio methods for the type of first and second row systems studied here.[13] All geometries are fully optimized using medium size basis sets, while the final energies are obtained using very large basis sets. For benchmark tests comprising 55 common first and second row molecules performed using slightly larger basis sets, an average absolute deviation compared to experiments of 2.2 kcal/mol was obtained for the atomization energies, of 0.013 Å for the bond distances and of 0.62° for the bond angles. The present accuracy is almost as high as in this benchmark test and should be enough to discriminate between the different RNR substrate mechanisms tried. In most of the present model systems there are also hydrogen bonds present. Much less is known about the accuracy of the B3LYP method for these bonds but previous tests have not indicated any particular problems.[14]

(9) Lenz, R.; Giese, B. *J. Am. Chem. Soc.* **1997**, *119*, 2784−2794.
(10) Persson, A. L.; Eriksson, M.; Katterle, B.; Pötsch, S.; Sahlin, M.; Sjöberg, B.-M. *J. Biol. Chem.* **1997**, *272*, 31533−31541.
(11) Siegbahn, P. E. M.; Crabtree, R. H. *J. Am. Chem. Soc.* **1997**, *119*, 3103.
(12) Becke, A. D. *Phys. Rev.* **1988**, *A38*, 3098. Becke, A. D. *J. Chem. Phys.* **1993**, *98*, 1372. Becke, A. D. *J. Chem. Phys.* **1993**, *98*, 5648.
(13) Bauschlicher, C. W., Jr.; Ricca, A.; Partridge, H.; Langhoff, S. R. In *Recent Advances in Density Functional Methods*; Chong, D. P., Ed.; World Scientific Publishing Company:, Singapore, 1997; Part II, p 165.
(14) Pavlov, M.; Siegbahn, P. E. M.; Sandström, M. *J. Phys. Chem. A* **1998**, *102*, 219−228.

For example, the water dimer binding energy is found to be 2.8 kcal/mol using the B3LYP method with saturated basis sets compared to the experimental value of 3.6 ± 0.5 kcal/mol.[15] The very sensitive O−O distance is found to be 2.92 Å, at the same level of accuracy when compared to the experimental value of 2.98 Å.[16]

II. Computational Details

The calculations were performed in two steps. First, an optimization of the geometry was performed using the B3LYP method.[12] Double-ζ basis sets were used in this step. In the second step the energy was evaluated for the optimized geometry using very large basis sets including diffuse functions and with two polarization functions on each atom. The final energy evaluation was also performed at the B3LYP level. All calculations were made using the GAUSSIAN-94 program.[17]

The B3LYP functional can be written as[12,18]

$$F^{\mathrm{B3LYP}} = (1 - A)F_x^{\mathrm{Slater}} + AF_x^{\mathrm{HF}} + \mathrm{B}F_x^{\mathrm{Becke}} + CF_c^{\mathrm{LYP}} + (1 - C)F_c^{\mathrm{VWN}}$$

where F_x^{Slater} is the Slater exchange, F_x^{HF} is the Hartree−Fock exchange, F_x^{Becke} is the gradient part of the exchange functional of Becke,[12] F_c^{LYP} is the correlation functional of Lee, Yang, and Parr[19] and F_c^{VWN} is the correlation functional of Vosko, Wilk, and Nusair.[20] *A*, *B*, and *C* are the coefficients determined by Becke[12] using a fit to experimental heats of formation, but Becke did not use F_c^{VWN} and F_c^{LYP} in the expression above when the coefficients were determined, but used the correlation functionals of Perdew and Wang instead.[21]

The B3LYP energy calculations were for all the present RNR substrate models made using the large 6-311+G(2d,2p) basis sets in the GAUSSIAN-94 program. This basis set has two sets of polarization functions on all atoms, and also diffuse functions. In the B3LYP geometry optimizations a much smaller basis set, the d95 set of the Gaussian-94 program, was used for all first row atoms. Even though it has been shown[13] that the final energies are extremely insensitive to the quality of the geometry optimization, a slightly larger basis set was still used for sulfur. This basis set was the 6-311G(1d) basis which is of triple-ζ quality with one d polarization function added. The effects of the added d function was checked in a few cases and found to be very small for the final energies (calculated using the large basis set) but was somewhat larger for the geometries. A few exceptions to this general recipe for performing the calculations were made and these concerned the treatment of sulfur. Since it has been shown that the atomization energy of SO_2 is quite slowly converging with the basis set size on sulfur,[13] an even larger basis set, the 6-311+G(3df,2p) basis set, was used in a few cases, see subsection III.e. The addition of the extra f and d function had very small effects in general for the present systems. The largest effect was found for the S−S bond in S_2 $(CH_3)_2$ which increased by 1.4 kcal/mol. However, this effect was found to be almost perfectly canceled in the actual formation of the S−S bond for the RNR substrate, by other effects of increasing the basis set. On the basis of these basis set investigations it is concluded that the basis sets used are close to saturated for the present reactions. Any inaccuracies of the results should therefore come from the chemical models used or from the use of the B3LYP functional.

Zero-point vibrational and thermal effects were calculated at the Hartree−Fock level using the d95 basis set and were then scaled by 0.9 as usual. To calculate these effects at the Hartree−Fock level is 1 order of magnitude cheaper than to obtain them at the B3LYP level at present. In benchmark tests, it has not been found to be more accurate to obtain zero-point effects at the more expensive B3LYP level,[13,22] and in a few test cases the same experience was obtained here. The fact that B3LYP-optimized geometries are used for the zero-point determinations rather than Hartree−Fock optimized geometries should have only quite small effects on the results as tested in previous studies.[14] All energies discussed below include zero-point effects. Thermal effects are considered less accurately determined and are discussed separately in the text. When thermal effects are not included this corresponds to reactions at 0 K.

The dielectric effects from the surrounding protein were obtained using the self-consistent reaction field (SCRF) method.[23,24] This is one of the simplest models for treating long-range solvent effects and considers the solvent as a macroscopic continuum with a dielectric constant ϵ and the solute as filling a cavity in this continuous medium. In the present study the self-consistent isodensity polarized continuum model (SCI-PCM) as implemented in the GAUSSIAN-94 program has been used. In this method the solute cavity is determined self-consistently. The default isodensity value of 0.0004 e/B^3 was used, which has been found to yield volumes very close to the observed molar volumes. The dielectric constant of the protein is the main empirical parameter of the model and it was chosen to be equal to 4 in line with previous suggestions for proteins. This value corresponds to a dielectric constant of about 3 for the protein itself and of 80 for the water medium surrounding the protein. This choice has recently been found to give very good agreement with experiment for two different electron transfer processes in the bacterial photosynthetic system.[25] In the present case where neutral models are chosen throughout, the details of how the dielectric effects are computed are quite unimportant since the effects are found to be extremely small.

III. Results and Discussion

In this section the results of the model calculations are discussed. Each step of the substrate reaction is discussed in one subsection, starting with the step where the ribonucleotide substrate is activated and ending with the step where the deoxyribonucleotide product is formed. To make it easier to follow what is happening in each reaction, the numbering of the atoms will be kept as it is for the ribonucleotide, see Scheme 1. As an initial starting point for the calculations the sequence of steps suggested from experiments and shown in Scheme 2 was used. As will be seen, deviations from these suggestions were soon found necessary and the subsequent reactions can therefore not be identified in Scheme 2 but will be described later on in this section. The overall substrate reaction using the present models can be written as shown in reaction 1.

This reaction is calculated to be exothermic by 12.2 kcal/mol for separated reagents and products. However, when the energies of the different steps are added together, an exothermicity of 18.9 kcal/mol is actually obtained. The difference between these energies is due to differences in hydrogen bonding

(15) Curtiss, L. A.; Frurip, D. J.; Blander, M. *J. Chem. Phys.* **1979**, *71*, 2103.

(16) Dyke, T. R.; Mack, K. M.; Muenter, J. S. *J. Chem. Phys.* **1977**, *66*, 498.

(17) Frisch, M. J.; Trucks, G. W.; Schlegel, H. B.; Gill, P. M. W.; Johnson, B. G.; Robb, M. A.; Cheeseman, J. R.; Keith, T.; Petersson, G. A.; Montgomery, J. A.; Raghavachari, K.; Al-Laham, M. A.; Zakrzewski, V. G.; Ortiz, J. V.; Foresman, J. B.; Cioslowski, J.; Stefanov, B. B.; Nanayakkara, A.; Challacombe, M.; Peng, C. Y.; Ayala, P. Y.; Chen, W.; Wong, M. W.; Andres, J. L.; Replogle, E. S.; Gomperts, R.; Martin, R. L.; Fox, D. J.; Binkley, J. S.; Defrees, D. J.; Baker, J.; Stewart, J. P.; Head-Gordon, M.; Gonzalez, C.; Pople, J. A. *Gaussian 94 Revision B.2*; Gaussian Inc.: Pittsburgh, PA, 1995.

(18) Stevens, P. J.; Devlin, F. J.; Chablowski, C. F.; Frisch, M. J. *J. Phys Chem.* **1994**, *98*, 11623.

(19) Lee, C.; Yang, W.; Parr, R. G. *Phys. Rev.* **1988**, *B37*, 785.

(20) Vosko, S. H.; Wilk, L.; Nusair, M. *Can. J. Phys.* **1980**, *58*, 1200.

(21) Perdew J. P.; Wang, Y. *Phys. Rev. B* **1992**, *45*, 13244. Perdew, J. P. In *Electronic Structure of Solids*; Ziesche, P., Eischrig, H., Eds.; Akademie Verlag: Berlin, 1991. Perdew, J. P.; Chevary, J. A.; Vosko, S. H.; Jackson, K. A.; Pederson, M. R.; Singh, D. J.; Fiolhais, C. *Phys. Rev. B* **1992**, *46*, 6671.

(22) Curtiss, L. A.; Raghavachari, K.; Redfern, P. C.; Pople, J. A. *Chem. Phys. Lett.* **1997**, *270*, 419.

(23) Wiberg, K. B.; Rablen, P. R.; Rush, D. J.; Keith, T. A. *J. Am. Chem. Soc.* **1995**, *117*, 4261. Wiberg, K. B.; Keith, T. A.; Frisch, M. J.; Murcko, M. *J. Phys. Chem.* **1995**, *99*, 9072.

(24) Dillet, V.; Rinaldi, D.; Rivail, J.-L. *J. Phys. Chem.* **1994**, *98*, 5034.

(25) Blomberg, M. R. A.; Siegbahn, P. E. M.; Babcock, G. T. *J. Am. Chem. Soc.* In press.

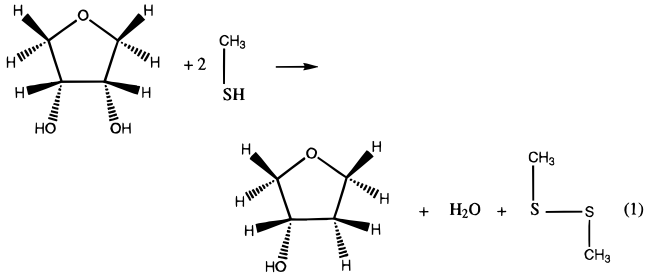

(1)

before and after the reaction. In particular, there is a strong hydrogen bonding with substantial protonic character to the product $S_2(CH_3)_2$, as will be described below.

Before the model results are discussed, a few comments should be given on the underlying principles used in setting up these models. A major, and unconventional, point is that all models are chosen to be neutral. This is done because previous model calculations have shown that this type of model mimics the real situation best. For example, in a model study of the Wacker process (olefin conversion to acetaldehyde catalyzed by palladium dichloride) performed recently,[26] it was shown that conventional models where a negatively charged hydroxyl anion attacks the coordinated olefin lead to very poor agreement with experimental findings. Much better agreement is obtained when neutral water molecules are used instead. The effects of long-range polarization can be added on afterward. For the present reactions these effects were found to be very small. The Wacker process, taking place in water, is an extreme comparison to the present reactions, since charge separations should be much larger in that case than they are here. In general for proteins, where the effective dielectric constant is low ($\epsilon = 4$), charge separations should be quite small as long as the protein is not specifically set up to create a charge separation as is the case for photosynthesis, for example, where the charge separation is necessary for ATP synthesis. There is no such requirement here and the models can therefore be assumed to be neutral. Minor charge separations will take place inside the models as will be seen below. Ultimately, the adequacy of the models can only be judged by the agreement or disagreement with experimental findings, such as measured rates and energetics.

a. Step 1. Hydrogen Atom Abstraction by the Cys439 Radical. The apparently simplest step of the reactions in Scheme 2 is the first one, where the Cys439 radical is suggested to abstract a hydrogen atom from the C3′-carbon of the ribonucleotide substrate. For this step there is essentially full agreement between the present calculations and Scheme 2. Three different models were tried: first without any additional amino acid residues, second with a model of Glu441, and third with a model also of Asn437. To model Glu441 a neutral formic acid is used in line with the arguments given above, and to model Asn437, a formamide group is used. The cysteine is modeled by an $HSCH_3$ group and the ribonucleotide by a ribose ($C_4H_6O(OH)_2$) molecule. This reaction step can be written as in reaction 2.

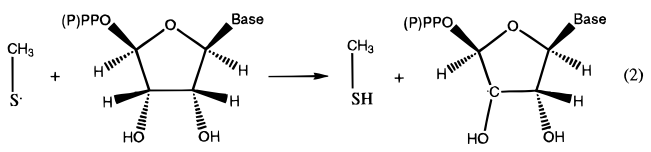

(2)

The results for the model without additional amino acid residues are as expected. Since the S−H bond strength in cysteine is weaker than the C3′-H bond in the ribonucleotide, reaction 2 is endothermic. The bond strengths calculated for the isolated ribose and $HSCH_3$ models are 89.4 and 83.5 kcal/mol, respectively. For reaction 2 the calculated barrier height is 9.2 kcal/mol and the endothermicity 5.9 kcal/mol using the model without the additional amino acid residues. The endothermicity is calculated as the difference in C−H and S−H bond strengths, rather than as a difference between the weakly hydrogen bonded complexes of the reactants and of the products, since the modeling of these weak interactions is rather uncertain. The difference between these procedures is in any case quite small for the present systems (on the order of 1 kcal/mol). These results show that the hydrogen abstraction by the cysteinyl radical is perfectly feasible with a rate on the order of 10^6 s^{-1} and that the reaction is endothermic as expected. The temperature effects on the barrier and endothermicity are small, in the range 0.5−1.0 kcal/mol, increasing the barrier and lowering the endothermicity. The dielectric effects from the surrounding protein are also small in the same range, with a decrease of 0.2 kcal/mol for the barrier and an increase of 0.8 kcal/mol for the endothermicity. In summary, there is thus full agreement with expectations based on experiments and no further model calculations for this reaction would appear necessary.

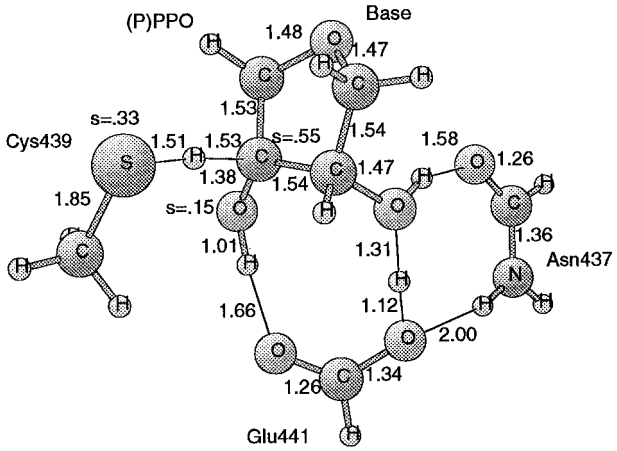

Figure 2. Optimized transition-state structure for hydrogen abstraction in step 1 according to reaction 2, including Glu441 and Asn437

In the initial phase of the present project (the first 50 geometry optimizations), the results for the model without any additional amino acid residues were considered as more or less final for this step. However, much more involved models were eventually found necessary to explore for the subsequent steps of the substrate reactions. The reasons for this will be described in detail in the coming subsections. At the moment it will suffice to mention that the Glu441 residue is found absolutely essential for some other steps and that the addition of Asn437 also has important consequences. Therefore, at the end of the project, the effects of adding these residues were also considered for the first step. When the glutamic acid model is added it will form hydrogen bonds both to the C3′-OH and C2′-OH groups as expected and when the asparagine model is also added the structure shown in Figure 2 is obtained for the transition state. It should be noted that the hydrogen bonding in this structure differs somewhat from what is found in the recent X-ray structure.[4] This will be discussed more below in the next subsection. There are some notable features of the structure in Figure 2. While the first hydrogen bond to the C3′-OH group is essentially normal with a hydrogen-bond distance of 1.66 Å, the hydrogen bonding to the C2′-OH is much stronger, with O−H bond distances of 1.12 and 1.31 Å. Without Asn437 these distances are 1.05 and 1.51 Å, so the asparagine effects are

(26) Siegbahn, P. E. M. *J. Phys. Chem.* **1996**, *100*, 14672.

Table 1. Effects (kcal/mol) of Adding Additional Amino Acid Residues to Reaction 2

additional residue	C−H bond strength	reaction energy	barrier height
no	89.4	5.9	9.2
Glu441	87.2	3.7	−
Glu441, Asn437	85.7	2.2	7.2

substantial. For the product of the C3′-H abstraction, the hydrogen-bonding effects are even more pronounced. The proton at the C2′-OH site is now between the two oxygens with distances of 1.22 and 1.20 Å. The hydrogen-bond distance has also shortened at the other OH site from 1.78 Å before the reaction to 1.62 Å afterward. The C3′-OH and the C2′-OH distances are now also substantially different at 1.37 and 1.53 Å, respectively. Before the abstraction these distances are 1.43 and 1.47 Å, respectively. Overall, these distance changes indicate that the abstraction of the C3′-hydrogen atom has initiated the release of the C2′-OH group. In fact, the next step of the substrate reactions, to be discussed in the next subsection, is thus already halfway complete. The spin distribution for the transition-state structure is essentially as expected with the spin mainly divided between sulfur and carbon. The spin populations are 0.33 for sulfur and 0.55 for carbon, but there is also some spin, 0.15, on the oxygen bound to C3′.

As expected from the rather large geometric effects of the addition of Glu441 and Asn437, there are also some energetic effects on the C3′-H abstraction reaction, see Table 1. Since the product of the hydrogen abstraction is more stabilized than the reactant, the C3′-H bond strength is weakened by the addition of these residues. Adding first Glu441 weakens the C3′-H bond strength by 2.2 kcal/mol and also adding the Asn437 leads to a further weakening by 1.5 kcal/mol. The overall reaction endothermicity for C3′-H abstraction is thus reduced by as much as 3.7 kcal/mol to 2.2 kcal/mol. There are also some effects on the barrier for the abstraction. With the addition of Glu441 and Asn437 the barrier is lowered by 2.0 kcal/mol, from 9.2 to 7.2 kcal/mol, leading to a rate of 10^7 s^{-1}. The effects on the endothermicity, in particular, are important when possible substrate radicals are identified following site-directed mutagenesis.[10]

In the initial model studies of reaction 2 simpler models for the ribonucleotide using a dihydroxyethane ($C_2H_4(OH)_2$) group and for cysteine using H_2S were tried. Both these simplifications have rather small, but still significant enough, effects on the energetics that they were not used further in this study. The effects of the simpler modeling of the ribonucleotide was a lowering of the barrier for hydrogen abstraction by 3.2 kcal/mol and a decrease of the endothermicity for reaction 2 by 1.9 kcal/mol. The effects of using H_2S as a model for cysteine were somewhat larger. Since the S−H bond strength is 4.8 kcal/mol weaker for $HSCH_3$ than for H_2S, 83.5 kcal/mol compared to 88.3 kcal/mol, this has a corresponding effect on reaction 2, where the endothermicity goes down from 5.9 to 1.1 kcal/mol, and the barrier from 9.2 to 3.4 kcal/mol. The experimental values for the S−H bond strengths of $HSCH_3$ and H_2S are 87.3 and 91.2 kcal/mol, respectively, showing that the bond strength difference is quite well-reproduced by the calculations but that the bond strengths are too weak, which is a typical result for these types of bonds at the B3LYP level.

An important technical point is that there are several isomers both of ribose and of its radical with well-defined minima that depend on the cis or trans orientations of the three oxygens. These are true minima without any imaginary vibrational frequencies. The OH bonds of the hydroxyl groups can point toward or away from each other, and the ring oxygen can point in the same or in a different direction than the hydroxyl groups with respect to the ring plane. The energy differences between these minima are in the range 1−3 kcal/mol. If the wrong minima are found before or after the reactions, relative errors of up to 5 kcal/mol can thus appear when different reactions are compared. In the above comparisons of energies when Glu441 and Asn437 were added, it was therefore carefully verified that the correct lowest minima were compared.

b. Step 2. Abstraction of the Hydroxyl Group Bound to C2′. In the first step of the substrate reactions there is thus very good agreement between the present calculations and the reactions in Scheme 2, even though the rather large effects of the Glu441 and Asn437 residues have not been suggested before for this step. However, in the second step there will already be major deviations from the reactions of Scheme 2. In this step, it was suggested that a proton should be abstracted by the C2′-hydroxyl group from a cysteine, either Cys225 or Cys462. On the basis of previous experience from calculations on reactions of this kind,[26] this reaction is already unlikely since it would lead to a large charge separation. A charge separation with a proton on the ribose group and a negative charge on the cysteine would require both a larger dielectric effect and a set of nearby water molecules to stabilize the charge separation, neither of them present here. Model calculations (without additional amino acid residues) support these expectations. The hydrogen abstraction reaction without a charge separation can be written:

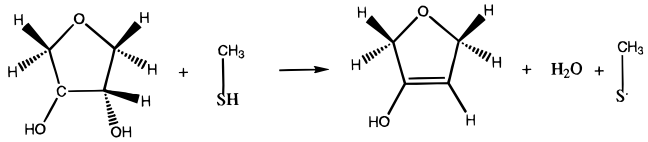

(3)

When this reaction is studied by the present theoretical methods, the possibility indicated in step 2 in Scheme 2 is automatically included. This would mean that the cysteine should become an anion rather than a radical and that a positive charge should reside on the complex between ribose and water. As expected, this did not occur, and the lowest energy barrier was instead found for a radical mechanism. The transition state for this reaction is shown in Figure 3, and the calculated barrier height is 16.2 kcal/mol. Since the starting point of reaction 3 is 5.9 kcal/mol above the starting point of reaction 2 (without additional amino acid residues), the transition state for reaction 3 is 22.1 kcal/mol above the starting point of the substrate reactions. This is much too high a barrier, leading to a predicted rate of only 10^{-3} s^{-1}, and reaction 3 therefore has to be ruled out. The reaction energy of reaction 3 is +3.5 kcal/mol, leading to a total endothermicity with respect to the starting point of the substrate reactions of 9.4 kcal/mol.

From the above it is clear that another reaction step than the one previously suggested is needed following step 1. One possibility suggested by previous model calculations is a direct pathway moving a hydrogen from the C3′-OH group over to the C2′-OH group to form water and an oxaallylic radical as shown in reaction 4.

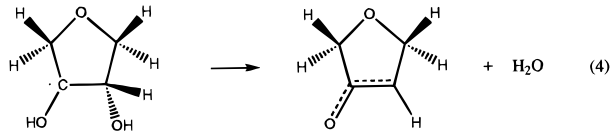

(4)

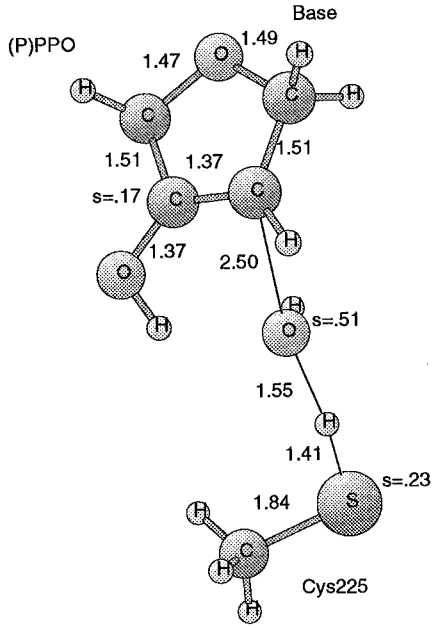

Figure 3. Optimized transition-state structure for hydroxyl abstraction in step 2 according to reaction 3

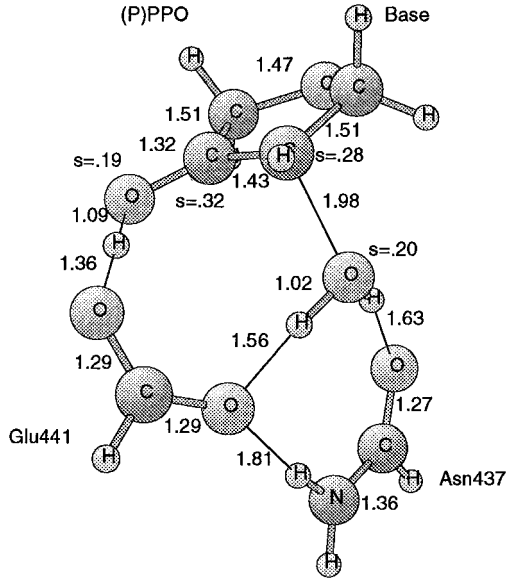

Figure 4. Optimized transition-state structure for hydroxyl abstraction in step 2 according to reaction 4, including Glu441 and Asn437

In the study of the Wacker process mentioned previously,[26] a reaction with some similarities to this reaction was found. The tautomerization from vinyl alcohol (C_2H_3OH) to acetaldehyde (CH_3CHO) was accomplished with a rather low barrier by bridging the carbon and oxygen sites by two water molecules and moving the hydrogen atom along the hydrogen-bonded water chain. In the present case the Glu441 residue is present containing the carboxylate group which should be ideal for this type of hydrogen transfer. Indeed, placing the Glu441 (modeled by a neutral formic acid as before) with its two carboxylic oxygens so that hydrogen bonds can be formed with the hydroxyl groups of the ribosyl radical, see Figure 4, leads to a very efficient transfer of a hydrogen atom from one hydroxyl to the other. Reaction 4 with the addition of the Glu441 model is calculated to be exothermic by 11.0 kcal/mol and has a barrier of only 4.9 kcal/mol, to be compared to an endothermicity of 3.5 kcal/mol and a barrier of 16.2 kcal/mol for reaction 3.

In the presently suggested reaction sequence, the Glu441 residue thus plays a key role by transferring a hydrogen atom from the C3′-OH site to the C2′-OH site. It is interesting to note in this context that the carboxylate function at position 441 has very recently been shown by site-directed mutagenesis to be essential for keeping turnover activity.[10] From that study it was suggested that the step where water is formed, step 3 in Scheme 2, is considerably slowed if there is no carboxylic group present. In the only mutation to retain turnover activity, the glutamic acid was replaced by an aspartic acid. When Glu441 was replaced by a glutamine, a new radical was seen suggested to be the C3′-radical formed after step 1. From the present study, this appears to be a reasonable suggestion but further calculations and experiments are needed to prove if this is the case. When the glutamate was replaced by a glutamine it was also shown that the reactions are eventually stalled at a later step, see further below.

At the transition state for the transfer of the hydrogen from the C3′-OH to the C2′-OH site, the hydrogen atom at the latter site is quite protonic. A reasonable question is therefore if the Asn437 residue, which is rather basic and also present in this region, could help to stabilize this transition state further. The transition state obtained when the formamide model of Asn437 is included is shown in Figure 4. As expected, the Asn437 residue stabilizes the transition state further and now this reaction step hardly has a barrier at all, only 0.3 kcal/mol. This means that the overall barrier, counting from the start of step 1, is 2.5 kcal/mol, leading to a predicted rate of 10^{10} s^{-1}. The reaction exothermicity on the other hand is almost the same as before the addition of Asn437, 10.7 kcal/mol compared to 11.0 kcal/mol. This shows that the protonic character of the hydrogen being transferred does not remain after the reaction. The spin populations for the transition state structure in Figure 4 show that the spin is quite delocalized. The spin population on C2′ is 0.28; on C3′, 0.32; on the C2′-oxygen, 0.20; and on the C3′-oxygen, 0.19. The ability to delocalize the spin may be one reason the barrier for this reaction is so low. In contrast, the transition state in Figure 3 which has a much higher barrier, also has most of the spin, 0.51, localized on one oxygen atom. The product of the reaction going over the transition state in Figure 4, the oxaallylic radical, has most of its spin, 0.67, on C2′ but there is also some spin, 0.26, on the C3′-oxygen. The temperature effects on the second step are also rather small, 0.5 kcal/mol for the barrier and 1.8 kcal/mol increase of the exothermicity. The dielectric protein effects are an increase of 0.8 kcal/mol for the barrier and a decrease of 0.6 kcal/mol for the exothermicity. One additional comment, regarding the geometry of the transition state, should also be made. The rather large energetic effect of adding the Asn437 residue does not show very clearly from the structure in Figure 4 with rather long hydrogen-bond distances of 1.63 and 1.81 Å, at least in comparison to the hydrogen-bond distances to the carboxylic group. Also, the nitrogen end of Asn437 might have been expected to be more directly connected with the proton being transferred. However, as will be discussed more in detail for step 4 below, this position of the Asn437 is the optimal one. One reason for this is that the most basic site of an asparagine is not the nitrogen but the oxygen end. The proton affinity on nitrogen is 179.3 kcal/mol, while the one on oxygen is 194.5 kcal/mol.

With the large energetic effect of Glu441 and Asn437, it is important that the positions of both residues in Figure 4 are consistent with their positions in the X-ray structures (3-Å resolution),[3,4] see Figure 1. It can be seen that their general

positions are indeed correct. However, there are some important deviations concerning their exact positions with regard to the hydrogen bonding, for example. A notable difference is that in the recent X-ray structure including the substrate, the amino end of the Asn437 residue is part of the cyclic hydrogen-bonding structure connecting the two hydroxyl groups, while for the present transition state Asn437 is outside this cycle, see Figure 4. To test the importance of this difference the transition state was also determined with a structure exactly corresponding to the X-ray structure. For a model complex consisting of the simpler 1,2-dihydroxyethyl radical rather than the ribose model, the transition state including the amino group in the cycle turned out to be as much as 9.1 kcal/mol higher than the one corresponding to Figure 4. This does, of course, not mean that the present model is inconsistent with the X-ray structure, but rather means that a slight rearrangement of hydrogen bonding is necessary before the reaction takes place. This rearrangement could take place just before step 2 or even before step 1, since the hydrogen-bonding properties of the substrate should change significantly already when Cys439 becomes a radical, as discussed in the preceding subsection. Some rearrangement of hydrogen bonds is not unexpected in this type of energy-demanding reactions since hydrogen bonds are rather weak and easy to exchange. The amino acid residues also are very flexibly bound and should be easy to move. As an example of the flexibility, a recent experimental study of the bacterial photosynthetic center showed that the quinones move over distances of 5 Å between their charged and charge-neutral positions.[27] In the X-ray structure of the RNR substrate region it is also shown that one of the cysteines moves 6.5 Å upon reduction.[4]

It is interesting to compare the present findings with those from the recent experimental study by Lenz and Giese.[9] They found that once a C3′-radical is made, elimination of the C2′-OH group readily takes place under general base catalysis. They suggest that the Glu441 residue is the key catalyst for this reaction. Their findings are thus perfectly in line with the present results, even though the description of what occurs is somewhat different. In their model they assume that Glu441 has already lost a proton before the reaction and that the remaining carboxylate anion should act as a base and abstract a proton from the substrate. In the present study the presence of well-separated charged ions is considered unlikely and neutral models are therefore used throughout. From the present results it is at least clear that charged ions are not needed to catalyze the substrate reactions. In fact, these results suggest that the reactions studied by Lenz and Giese are better described by models such as those in Figure 4. In the modified scheme of Stubbe et al.,[8] they also indicate a role of Glu441 but the donation of a proton from a cysteine to form water is kept, which is different from the present scheme.

Another quite recent study has clear connections to the present results for step 2 of the RNR substrate reactions. In a theoretical study George, Glusker, and Bock investigated the enzyme−coenzyme B_{12}-catalyzed dehydration of 1,2-dihydroxyethane.[28] Since this reaction is initiated by a hydrogen abstraction from a carbon center, that reaction becomes extremely similar to step 2 of the present reactions. In their study, charged models were mostly used. The present results suggest that a carboxylate-containing amino acid, such as a glutamic or aspartic acid, should easily catalyze the dehydration of the dihydroxyethane. It is most probably important to use neutral models also in that case.

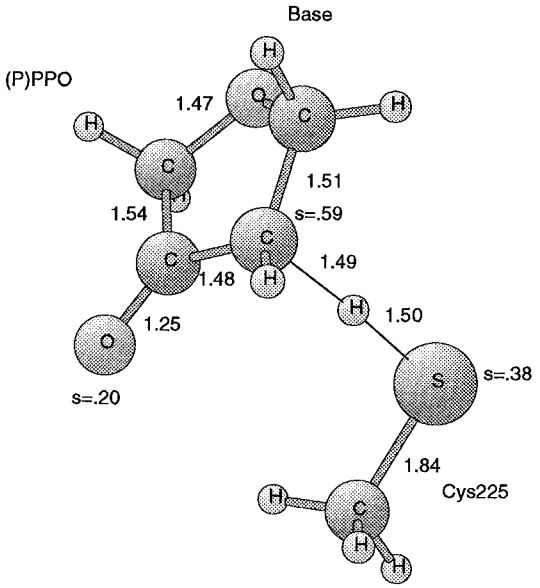

Figure 5. Optimized transition-state structure for ketone formation in step 3 according to reaction 5

c. Step 3. Formation of a Ketone by Hydrogen Abstraction. With the abstraction of the C2′-OH group, one of the most problematic steps in the transformation from a ribonucleotide to a deoxyribonucleotide has been performed. The next step, step 3, is then a rather trivial reaction with few alternatives. Starting out from the oxaallylic radical formed after the transition state in Figure 4, a stable nonradical ketone can be obtained simply by C2′-abstraction of a hydrogen from one of the nearby cysteines, either Cys225 or Cys462. From the X-ray structures, Cys225 is better positioned for this abstraction, and this will therefore be assumed in the following. This reaction is thus quite similar to the reverse of the first step and can be written as in reaction 5.

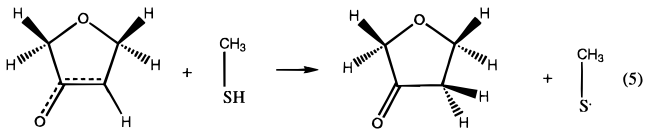

(5)

The calculated barrier for this reaction is 7.4 kcal/mol and the exothermicity 4.2 kcal/mol. The reaction rate should thus be 10^7 s^{-1} and would be far from rate-limiting for the RNR transformation. The temperature effects (compared to 0 K) are predicted to be an increase of 1.5 kcal/mol for the barrier and a decrease of 0.4 kcal/mol for the exothermicity. The dielectric effects (as compared to the system placed in a vacuum) are a decrease of 0.1 kcal/mol for the barrier and a decrease of 1.0 kcal/mol for the exothermicity. Some investigations were made of possible hydrogen-bonding effects similar to those of the first step, but no significant effects were found (less than one kcal/mol). The optimized transition state is shown in Figure 5. The spin populations are as expected divided between sulfur and the C2′-carbon, with values of 0.38 and 0.59. An alternative hydrogen abstraction to the one described in reaction 5 would be one where the hydrogen would be abstracted by the oxygen. However, the alcohol product of this abstraction is found to be 12.5 kcal/mol less stable than the keto product in Figure 5.

Since in the present scheme, step 3 is the first step where Cys225 should be active in the reactions, it is interesting at this

(27) Stowell, M. H. B.; McPhillips, T. M.; Rees, D. C.; Soltis, S. M.; Abresch, E.; Feher, G. *Science* **1997**, *276*, 812.

(28) George, P.; Glusker, J. P.; Bock, C. W. *J. Am. Chem. Soc.* **1997**, *119*, 7065.

stage to relate the present results to site-directed mutagenesis experiments where Cys225 has been replaced by a serine residue.[29] The main difference between cysteine and serine in the present context is that the S−H bond strength of cysteine, 83.5 kcal/mol (calculated), is much weaker than any of the C−H or O−H bond strengths of serine, which should all be stronger than 100 kcal/mol. It is therefore predicted that the RNR reaction sequence should be stalled after the formation of the oxaallylic radical in step 2 if the hydrogen abstraction from Cys225 cannot be made. In the experiments the C225S mutation leads to a complicated set of reactions that eventually lead to the cleavage of the polypeptide into two new polypeptides. This reaction sequence is probably even more complicated than the original RNR sequence, and it is clearly not possible to explain the experimental observations solely based on the present calculations. However, a few remarks can be made. The first remark is that the C−H bond formed when the oxaallylic radical abstracts a hydrogen atom is as strong as 87.3 kcal/mol (calculated). This means that an attack on the polypeptide may well be possible. In further support for this type of reaction, the RNR sequence as suggested here does not easily go backward, at least not beyond step 1. The barrier for going backward is 15.7 kcal/mol which corresponds to a reaction rate of only 10 s^{-1}. An alternative to the attack on the polypeptide is, of course, a hydrogen abstraction from Cys439. In the experimental analysis this is the explanation used for the observation that multiple uracils are produced per Tyr122 radical lost. It is interesting to note that this process requires that Cys439 can access both the C2′ and C3′ carbons. In the present reaction scheme, this type of flexibility is required for Cys225 instead, in step 4, see next subsection. In summary, even though the reactions observed by the C225S mutation are too complicated to be rationalized by the present calculations, the present RNR reaction sequence, with a powerful oxaallylic radical formed which does not easily return backward in the sequence, is at least consistent with the observations made.

d. Step 4. The attack on the C3′-Center. To find a mechanism with a reasonable barrier for step 4 turned out to be the by far most difficult problem in the present study. A large number of possibilities were tried, including about 50 different geometry optimizations with models with up to 35 atoms, before the most plausible reaction was found. Only a few of the alternatives tried will be described here.

The first, and obvious, result obtained in the investigations of a possible fourth step is that a hydrogen abstraction of the type found in steps 1 and 3 is not possible. The oxygen of the ketone binds a hydrogen atom by only 22.3 kcal/mol, while a hydrogen atom is bound to a cysteine by 83.5 kcal/mol, leading to an endothermicity of 61.2 kcal/mol for such a reaction. A more interesting possibility is that the Cys225• radical, released after step 3, could add to the ketone. There are two different possibilities. First, the addition of the SCH_3• radical to the keto oxygen is found to be endothermic by 28.2 kcal/mol. Second, adding SCH_3• to C3′ is endothermic by 15.3 kcal/mol. Both these possibilities can therefore be ruled out as possible intermediates for further transformations on the way to the deoxyribonucleotide product. A slightly more interesting possibility is that a rearrangement takes place, in which a hydrogen moves from C2′ to the keto oxygen and that the SCH_3• then binds to C2′. The structure obtained is 10.9 kcal/mol less stable than the isolated ketone and the Cys225• radical, and is also ruled out.

(29) Mao, S. S.; Holler, T. P.; Bollinger, J. M.; Yu, G. X.; Johnston, M. I.; Stubbe, J. *Biochemistry* **1992**, *31*, 9744−9751.

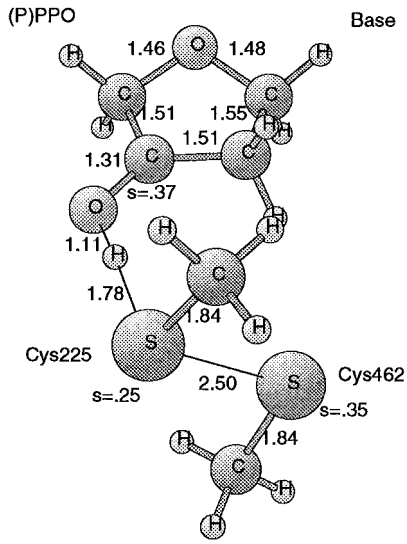

Figure 6. Optimized transition-state structure for disulfide formation in step 4 according to reaction 6

A much more plausible step than those mentioned above, is that a hydrogen abstraction by the ketone occurs simultaneously as a disulfide bond is formed as described in reaction 6. The

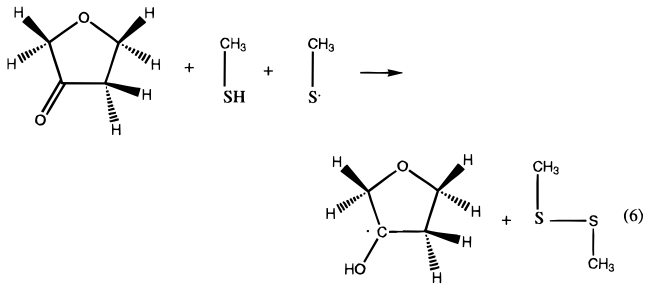

hydrogen atom should then be abstracted by the keto oxygen with a simultaneous formation of a disulfide bond. To make this mechanism consistent with the recent X-ray structure, a hydrogen atom first has to be abstracted from Cys462 by Cys225. This is necessary because Cys462 is too far away from the substrate to directly interact with it. The hydrogen atom abstracted by the keto oxygen will then come from Cys225 instead and the disulfide bond will be formed between Cys225 and the Cys462• radical. This reaction is endothermic by 7.0 kcal/mol, which does not rule out the product as a possible intermediate. However, the barrier for the reaction is as high as 24.5 kcal/mol, which is too high. The transition state for this reaction is shown in Figure 6. Attempts to find a similar transition state, but where the hydrogen atom is abstracted by C3′, led back to the transition state in Figure 6. Different types of concerted reactions were also tried. For example, the disulfide bond formation was combined with reaction 5 or with a hydrogen abstraction by C3′ from Cys439. These attempts all led back to nonconcerted reactions. Several other unsuccessful attempts of similar reactions were also made.

At this stage, with several unsuccessful attempts to attack the very stable ketone formed after step 3, the possibility that step 3 is actually a dead end was considered by trying to find reaction paths leading directly from the oxaallylic radical formed in step 2, further toward the deoxyribonucleotide. These reaction paths could also be ruled out. In an attempt to find a way out of this dilemma, a possible product of an addition reaction between the ketone and $HSCH_3$ was located. The only reasonable such product is with the hydrogen bound to the keto

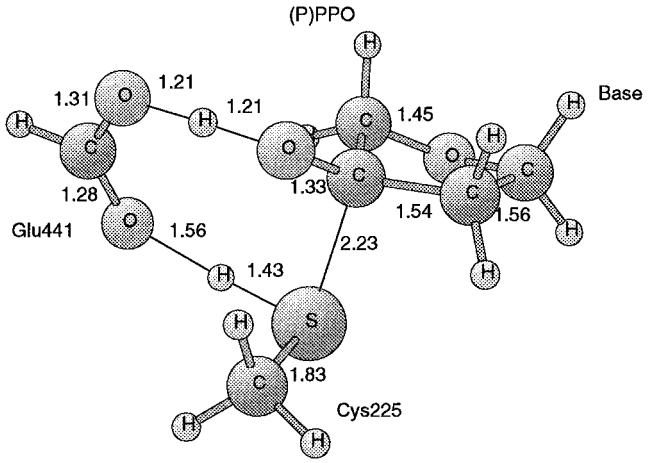

Figure 7. Optimized transition-state structure for cysteine attack on C3′ in step 4 according to reaction 7, including Glu441

oxygen and with the SCH_3 group bound to C3′. This nonradical reaction can be written as in reaction 7.

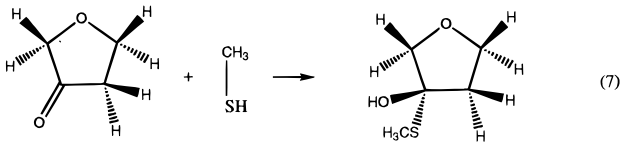

(7)

Reaction 7 turns out to be endothermic by only 2.7 kcal/mol and indicates that the product could be a possible intermediate in the deoxyribonucleotide synthesis. However, the barrier for reaction 7 is as high as 41.2 kcal/mol, which means that a quite different attack than the direct one has to be found to form the product, if it should remain a possible reaction step.

A confirmation that a reaction like 7 could be possible is found by the fact that acetaldehyde is known to be unstable in water leading to an analogous product as in reaction 7. A proton attacks the keto oxygen and a hydroxyl anion attacks the keto carbon in an acid-catalyzed reaction. A large number of model reactions were then set up to try to describe this simpler acetaldehyde reaction. These models were based on the same principles as the model used to describe step 2 and previously to describe the reactions in the Wacker process. A chain of water molecules was set up to bridge the two points of attack on the ketone, the carbon and the oxygen sites. Formic acid was also placed in the ring to model the acid catalyst. At the end of these investigations on acetaldehyde, new models could be suggested for step 4 of the RNR sequence. The first of these is shown in Figure 7, where again a hydrogen atom has been abstracted from Cys462 by Cys225 preceding the reaction in order to be consistent with the X-ray structure, where Cys462 is too far away from the substrate to interact with it. The presence of Glu441 in the ring bridging the oxygen and the carbon sites, significantly stabilizes the transition state. The barrier is decreased from 41.2 kcal/mol without Glu441 to 15.9 kcal/mol. However, this barrier would lead to a predicted rate of 10 s^{-1} which is hardly fast enough since this is the same order as the rate for an entire transformation from a ribonucleotide to a deoxyribonucleotide.

At this stage, where both Cys225 and Glu441 have been used, there is essentially only one possibility left, and this is to incorporate also Asn437 in the ring. To find a positive effect of Asn437, like the one for step 2, turned out to be harder than expected. Placing Asn437 with its nitrogen end in the ring between Cys225 and Glu441, gave a a large increase of the barrier height from 15.9 to 28.9 kcal/mol. A similar increase was found also for step 2 when an asparagine was incorporated into the ring. It should be noted that it is only the nitrogen end of the asparagine that can be placed in the ring since the oxygen end has no hydrogen to transfer. This is also the reason for the problem to obtain a positive effect by placing Asn437 directly in the ring. As already mentioned in the discussion of step 2, the proton affinity at the nitrogen end is not as high as the one on oxygen, 179.3 kcal/mol compared to 194.5 kcal/mol. Other positions for Asn437 in the ring were also tried, such as the position between Glu441 and the oxygen of the keto group, but without any lowering of the barrier height. Positions outside of the ring were also tried without success. It turns out that it is actually better to place a water molecule in the ring rather than an asparagine, which is also quite surprising. When a water molecule is placed in the ring the barrier height is 17.3 kcal/mol, which is higher than without the water but much lower than with the asparagine in the ring. Since the proton affinity of water is only 160.9 kcal/mol, which is 18.1 kcal/mol lower than the proton affinity of the nitrogen end of asparagine, it is thus clear that the proton affinity is not the only decisive factor for the efficiency of placing a molecule in the ring. A molecule in the ring has to be able to both accept and deliver protons, and apparently water is better than asparagine in this respect.

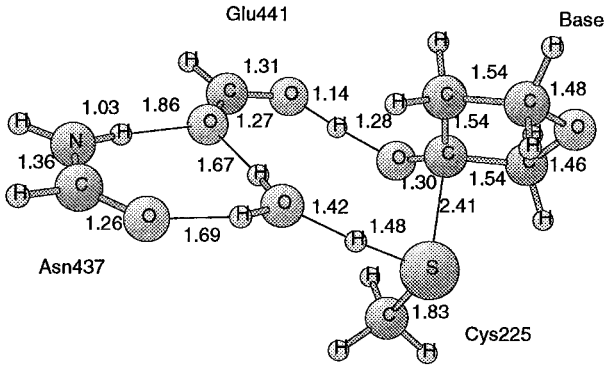

Figure 8. Optimized transition-state structure for cysteine attack on C3′ in step 4 according to reaction 7, including Glu441 and Asn437

Having placed water in the ring with only a small cost for the barrier in step 4, other possibilities to position asparagine are possible. One such possibility is shown in Figure 8, which also turns out to be the optimal position. An interesting aspect of this arrangement is that it is the same one as is created after step 2, and which is thus easily available for step 4. The water molecule in the ring emanates from the hydroxyl group abstracted from C2′ of the ribose ring. The barrier for the transition state in Figure 8 is 12.4 kcal/mol, leading to a predicted rate of 10^4 s^{-1}, which is clearly fast enough to be consistent with an overall rate of 10 s^{-1} for the entire RNR sequence. The step 4 reaction is computed to be endothermic by 1.8 kcal/mol.

The mechanism suggested by Lenz and Giese[9] for the attack on the C3′-keto group has both similarities and differences to the one suggested here. In their mechanism a proton from Glu441 is proposed to attack the oxygen and an electron is donated from a disulfide anion. The present scheme is similar but is more charge neutral, with a donation of a hydrogen atom to the oxygen from Glu441, a simultaneous acceptance of a hydrogen atom from Cys225, and a formation of a C−S bond. One difference between these schemes is that a disulfide anion is assumed formed prior to the attack on the C3′-keto group in the Lenz−Giese mechanism, while the sulfur−sulfur bond is formed only later in step 5, see below, in the present scheme.

In the presently suggested reaction sequence the attack on the C3′-keto group is the rate-limiting step. It is furthermore found that Glu441 is even more essential for this step than it is for the water formation in Step 2. It is interesting to note that these findings are exactly in line with the results of the recent site-directed mutagenesis experiment where the glutamate was substituted by a glutamine.[10] In that study it was found that the water formation step was significantly slowed by the mutation, in line with the essential role found here for Glu441 in this step. Furthermore, it was found that the reaction sequence would not go beyond the formation of the keto compound if there is no carboxylate group present, in line with the finding that this is the rate-limiting step and that Glu441 is essential also for this step.

The present suggestion for step 4 of the RNR sequence requires a quite flexible positioning of Cys225. The Cys225 residue must be able to reach both the C2′ carbon in step 3 and the C3′ carbon in step 4. In support for this possibility there are several observations of reactions where amino acid residues move over substantial distances, see further discussion for step 2. The site-directed mutagenesis experiment where Cys225 is replaced by a serine, is furthermore interpreted to show a similar flexibility of Cys439 to reach the two carbon centra.[29] On the other hand, the recent X-ray structure[4] does not indicate any such rearrangement, even though it can clearly not be ruled out on the basis of this structure alone. Likewise, the present calculations do not rule out possibilities that reaction pathways may eventually be found which require less motion of Cys225. A few such possibilities have already been tried, see further in the discussion of step 5.

Since the reaction in step 4 is the most critical one in the RNR sequence a few comments can be made at this stage on the expected accuracy of the calculations. The general performance of the B3LYP method has already been mentioned at the end of the introduction, but a few more details can be given. First, it is clear that even with such a small average deviation of calculated energies compared to experiment as 2.2 kcal/mol, a high accuracy on rates cannot be expected. For every 1.4 kcal/mol deviation on a barrier there will be an error on the rate of 1 order of magnitude. This means that the predicted rates can quite possibly deviate from experiments by 2 orders of magnitude. However, the goal of the present study is not to give accurate predictions of rates but to compare and distinguish different possible mechanisms, and in this case the error is not as serious as it may seem. On the basis of previous experience, it is very unusual that two different mechanisms differ in barrier heights by only a few kilocalories per mole, and this is true also in the case of the RNR mechanisms. Most conclusions concerning mechanisms can therefore be made even with an uncertainty in the rates of a few orders of magnitude. In the case of step 4, the prediction that the mechanism shown in Figure 8 in reality is also the best one of the mechanisms so far thought of is therefore quite certain, but the calculated rate of 10^4 s^{-1} is much more uncertain. In addition to this uncertainty of the B3LYP rate, there is also some uncertainty concerning the temperature effects. The calculated temperature effects (as compared to 0 K) indicate an increase of the barrier height by nearly 3 kcal/mol. This should mean a decrease of the rate by 2 orders of magnitude. This effect, which solely comes from the entropy, should ideally have been obtained using a more accurate Hessian than one obtained at the Hartree−Fock level, but this is too expensive at present for a system as large as this one. The Hartree−Fock Hessian could easily have severe problems for many of the low frequencies that are important for the entropy. At the present stage, the large entropy effect, much larger than for any other step discussed here, is considered unlikely. Only future studies will decide whether this is true or not. The dielectric effects from the protein (as compared to the system placed in a vacuum) are small with an increase of 0.9 kcal/mol for the barrier and an increase of 0.4 kcal/mol for the endothermicity.

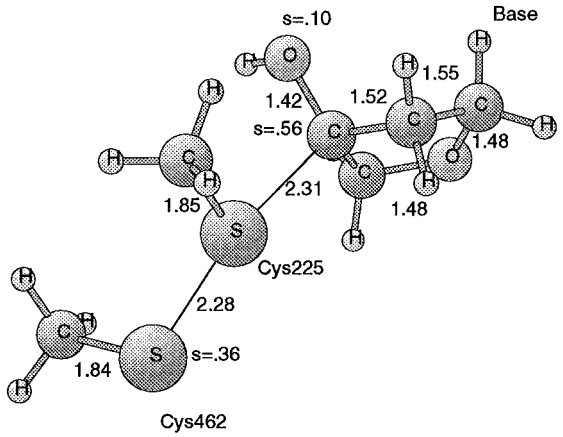

Figure 9. Optimized transition-state structure for disulfide formation in step 5 according to reaction 8

e. Step 5. The Formation of the Disulfide Bond. It is known from experiments that a disulfide bond is formed between Cys225 and Cys462 during the RNR sequence. In fact, the first X-ray structure of R1 was of a form where the disulfide bond was already present, see Figure 1. In the reaction sequence suggested from experiments, see Scheme 2, the disulfide bond is already formed in step 4, but in the presently suggested sequence this only occurs in step 5. As discussed above, all attempts to form a disulfide bond in step 4 were unsuccessful leading to too high barriers. The formation of the disulfide bond in step 5 should occur basically as described in reaction 8.

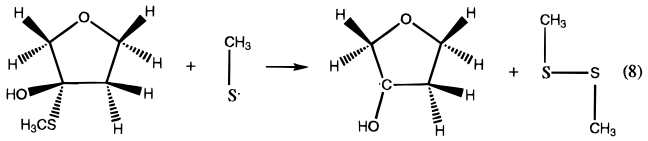

The straightforward calculation following reaction 8 leads to the transition state in Figure 9. The Cys462• radical formed prior to step 4 attacks the Cys225 residue bound to the C3′-carbon after step 4. The calculated barrier height for this reaction is 10.8 kcal/mol. Adding the 1.8 kcal/mol endothermicity of step 4, this means that the transition state in Figure 9 should be 12.6 kcal/mol higher than the starting point of step 4. This energy is almost the same as the energy of the transition state for step 4, and it must be possible to reach it if the transition state of step 4 is possible to reach. The predicted rate for this reaction should thus be 10^4 s^{-1}. Reaction 8 is furthermore calculated to be endothermic by 3.1 kcal/mol and should not constitute a major problem in the RNR sequence either. An additional test calculation was finally performed for this reaction. Since an S−S bond is formed in this step there could be an uncertainty concerning the adequacy of the 6-311+G(2d,2p) basis set. In particular, f functions on sulfur could turn out to be important since they were found to be quite important for the atomization energy of SO_2.[13] However, going to the larger 6-311+G(3df,2p) basis did not change the barrier height of reaction 8 by more than 0.2 kcal/mol. It is concluded that the basis set is saturated even for this more complicated reaction.

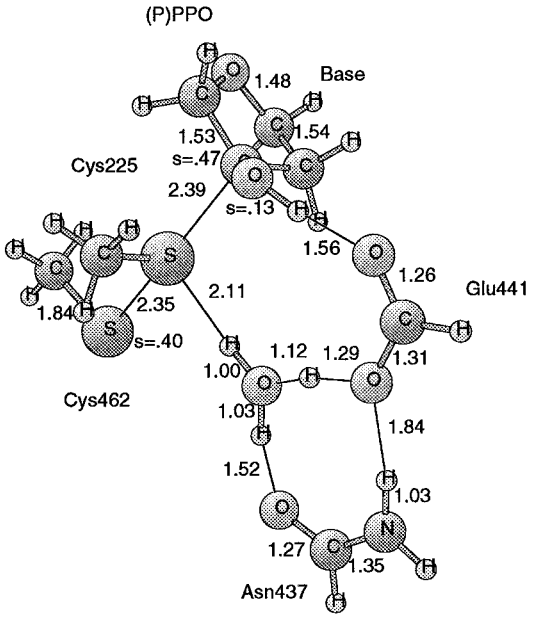

Figure 10. Optimized transition-state structure for disulfide formation in step 5 according to reaction 8, including Glu441 and Asn437

As in some of the previous steps, the effects of the Glu441 and Asn437 residues were also investigated for step 5. To be consistent with the products formed after step 4 (and after step 2), a water molecule was also included. These groups were placed as they appear at the end of step 4. Including these residues leads to the largest and most complicated transition state obtained in the present study. The optimized transition state is shown in Figure 10. One of the most interesting aspects of this structure is that an H_3O^+ can be identified and also an $HCOO^-$ anion. This shows that minor charge separations are indeed possible to describe within the present models. A charge separation does not have to be imposed on the system by assuming some residue to be ionized. Even with the charge separation in the structure in Figure 10, the long-range dielectric effects on the barrier are not expected to be large since the dipole moment only changes from 5.5 to 6.1 D from the reactants to the transition state. This is also shown by the dielectric cavity calculations where very small effects were obtained, see below. The calculated barrier is 6.4 kcal/mol, showing that the addition of Glu441 and Asn437 (and the water) lowers the barrier by 4.4 kcal/mol. This is a significant effect and it can be concluded that these residues are of importance in many steps of the RNR sequence. Adding the 1.8 kcal/mol endothermicity of step 4, the transition state in Figure 10 is 8.2 kcal/mol higher than the starting point of step 3. This leads to a predicted rate for this step of 10^7 s^{-1}, well in line with the overall rate of 10 s^{-1} for the overall RNR sequence. The calculated reaction endothermicity of reaction 8 including all residues is 0.2 kcal/mol. As mentioned in the beginning of this section the exothermicity in going from a ribonucleotide to a deoxyribonucleotide is increased from 12.2 kcal/mol for reaction 1 to 18.9 kcal/mol by additional hydrogen bonding on the product side. Part of this hydrogen bonding comes from this step where the partial transfer of a proton from Glu441 to the water molecule leads to a rather strong hydrogen bond to the disulfide. For the products of step 5, the proton is exactly between water and Glu441 with O−H distances of 1.20 Å. It is possible that this strong hydrogen bonding will also play a role when the disulfide bridge is reduced by thioredoxin and glutaredoxin, before the next catalytic cycle. The estimated temperature effects on step 5 are an increase of the barrier by 0.8 kcal/mol and an increase

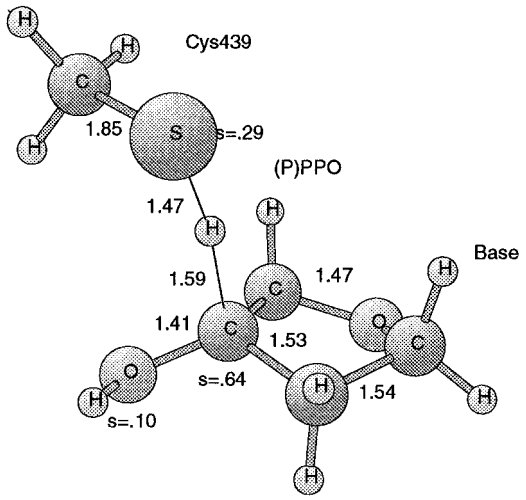

Figure 11. Optimized transition-state structure for deoxyribonucleotide formation in step 6 according to reaction 9

of the endothermicity by 1.8 kcal/mol. The dielectric effects from the protein are small with an increase of 0.2 kcal/mol for the barrier and an increase of 0.3 kcal/mol for the endothermicity. It should be noted that these effects are small using the present neutral models even though there are clear signs, see Figure 10, of the formation of both an H_3O^+ ion and a carboxylate anion. The spin populations for the transition-state structure in Figure 10 are a little bit surprising with no spin on the sulfur closest to C3′. Instead the other sulfur has a spin population of 0.40 and the C3′ carbon a spin population of 0.47.

Since the present reaction sequence requires a substantial flexibility of the Cys225 residue, it needs to reach both the C2′- and C3′-carbons, an alternative mechanism where this is avoided was also tried. In a combination of steps 4 and 5, the oxygen of the stable ketone formed in step 3 is attacked by a chain of amino acids in which Glu441 is inserted between the keto oxygen and Cys225 for the structure shown in Figure 6. By inserting Glu441, Cys225 is no longer forced to come close to the C3′ center. Without Glu441 the barrier for hydrogen abstraction (see step 3) is 24.5 kcal/mol, which is too high to be a realistic alternative. Inserting Glu441 actually increases the barrier by 2.8 kcal/mol to 27.3 kcal/mol. A mechanism where the movement of Cys225 is reduced will therefore require a quite different mechanism. It cannot be ruled out that such a possibility exists, but so far no such mechanism has been found.

f. Step 6. The Formation of the Deoxyribonucleotide. The final step of the RNR reaction sequence is, of course, the reverse of the first step as in reaction 9. A hydrogen atom should be abstracted by the C3′ center from Cys439. However, this does not mean that the energies of reactions 2 and 9 are the same. As discussed for step 1, both Glu441 and Asn437 play an important role in reaction 2 by initiating the water formation occurring in the second step, which reduces the endothermicity of step 1 by 3.7 kcal/mol. Any similar effect cannot occur for reaction 9 in step 6 since the C2′-hydroxyl group is no longer present. In fact, the effects of additional residues were found to be very small for reaction 9. The

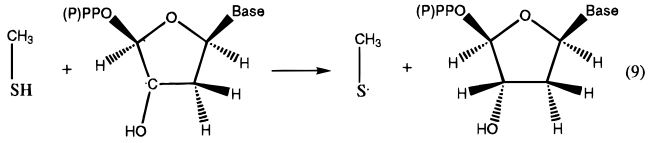

(9)

calculated barrier for step 6 passing over the transition state

Scheme 3. Proposed Reaction Scheme

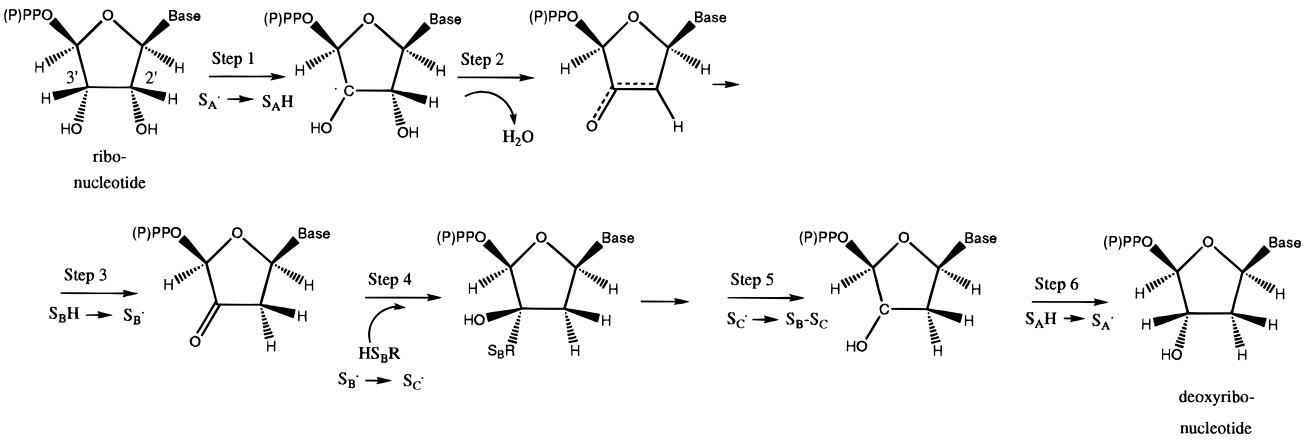

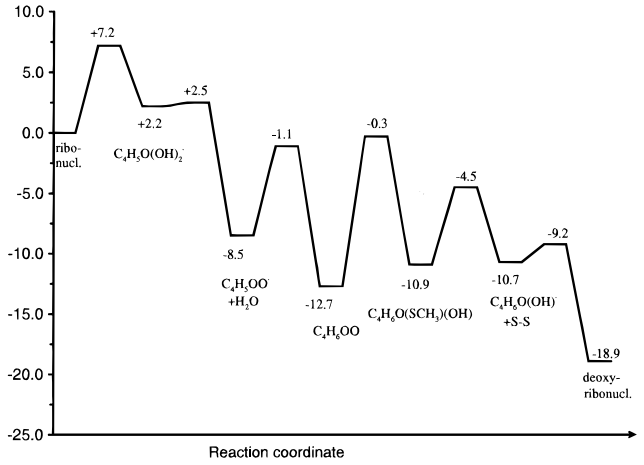

Figure 12. Energy diagram for the transformation from a ribonucleotide to a deoxyribonucleotide

structure shown in Figure 11 is 1.5 kcal/mol. The reaction is found to be exothermic by 8.2 kcal/mol. The individual effects on the exothermicity of adding first Glu441 and then also Asn437 were found to be less than one kcal/mol in opposite directions. The estimated temperature effects are an increase of the barrier by 1.6 kcal/mol and a decrease of the exothermicity by 0.4 kcal/mol. The dielectric effects from the protein are small with an increase of 0.3 kcal/mol for the barrier and a decrease of 0.4 kcal/mol for the exothermicity. The spin populations for the transition state are 0.29 on sulfur and 0.64 on carbon, quite similar to the ones for the transition state for step 1.

IV. Summary and Conclusions

The best pathway found for the transformation of a ribonucleotide to a deoxyribonucleotide by RNR occurs in six steps, see Scheme 3. The energy diagram for these six steps is shown in Figure 12. In step 1, which has a barrier of 7.2 kcal/mol and an endothermicity of 2.2 kcal/mol, a hydrogen atom is abstracted from C3′ of the ribose ring by Cys439. This abstraction is assisted by the presence of the Glu441 and Asn437 residues, which initiate the transfer of a hydrogen from the C3′-OH group to the C2′-OH. The completion of this transfer, leading to formation of a water molecule, occurs in the second step, which has a very small barrier of 0.3 kcal/mol and which is exothermic by 10.7 kcal/mol. This abstraction of the C2′-OH group is thus suggested to occur by a different mechanism than the one assumed until recently, see Scheme 2, where a cysteine residue was thought to be involved. However, it should be noted that the mechanism suggested here for this step is very similar to the one proposed recently by Lenz and Giese.[9] At the end of step 2 an oxaallylic radical is formed, and this is found to be the most stable of all the radicals formed in the RNR sequence, including those formed in R2. Still, if no mutations are made, this oxaallylic radical will be hard to observe experimentally since it can easily form an even more stable keto system. This is suggested to occur in step 3 where a hydrogen is abstracted by C2′ in the ribose ring from the Cys225 residue. The barrier for this step is 7.4 kcal/mol and the reaction is exothermic by 4.2 kcal/mol. The keto group is the most stable species formed so far in the RNR sequence and is the resting state for the remaining steps of the cycle.

To find a mechanism with a reasonable barrier for step 4 turned out to be very difficult. Several unsuccessful attempts were made to attack the stable keto group by combinations of the different amino acid residues present at the active site. The mechanism with the lowest barrier found is one where the Cys225 group attacks the C3′ center of the ribose ring. This is suggested to occur by a simultaneous formation of a C−S and an O−H bond at the C3′-keto group. However, a direct attack by Cys225 alone has a very high barrier. Instead, a cyclic transition state is proposed to be formed, see Figure 8, including apart from Cys225 also Glu441 and a water molecule in the ring, and an Asn437 residue outside the ring. This stabilizes the transition state sufficiently that it becomes a possible reaction step. The calculations indicate that this should be the rate-limiting step of the six substrate steps with a barrier of 12.4 kcal/mol and an endothermicity of 1.8 kcal/mol. This barrier corresponds to a rate of 10^4 s^{-1}, which should be fast enough since the overall reaction rate for formation of a deoxyribonucleotide is on the order of 10 s^{-1}. However, it should be noted that the theoretical prediction of rates has large uncertainties, about 2 orders of magnitude, since the rate depends exponentially on the barrier, and that there is also some uncertainty concerning the temperature effects. In the fifth step, the disulfide bond between Cys225 and Cys462 is suggested to be formed, assisted by the presence of Glu441 and Asn437, which leads to a barrier of 6.4 kcal/mol and an endothermicity of 0.2 kcal/mol. In the sixth step, the deoxyribonucleotide should finally be formed in essentially the reverse of the first step. A hydrogen atom is abstracted from Cys439 by the C3′ center with a barrier of 1.5 kcal/mol and an exothermicity of 8.2 kcal/mol. Altogether, this means that the formation of a deoxyribonucleotide from a ribonucleotide is calculated to be exothermic by 18.9 kcal/mol. The reason this is more than 12.2

kcal/mol calculated for the overall reaction 1 for the individual molecules is that additional hydrogen bonds are also formed in this process.

It should finally be noted that Scheme 3 is consistent with all site-directed mutagenesis experiments performed so far, even though these experiments did in fact not guide the present calculations at all. Particularly striking is the agreement with the recent experiments where the glutamate was engineered to alanine, aspartic acid, and glutamine.[10] For alanine there was no activity, for aspartic acid the activity was slightly reduced, and for the most interesting case of glutamine, the reaction was interpreted as stalled after the formation of the keto system. In the present scheme, the glutamate is found to be important in step 2, where water is formed, and in step 4 in the attack on the keto system, and the barriers for these steps are expected to be significantly raised if glutamate is changed to a glutamine. This should make step 2 slow but still possible, and the reaction sequence should entirely stop for the rate-limiting step 4 in very good agreement with the conclusions of the experimental paper.

Acknowledgment. I am very grateful to Robert Crabtree and Britt-Marie Sjöberg for valuable comments on the manuscript.

JA9736065